J Ginseng Res 39 (2015) 125–134

Contents lists available at ScienceDirect

Journal of Ginseng Research

journal homepage: http://www.ginsengres.org

Research article

Anti-breast cancer activity of Fine Black ginseng (*Panax ginseng* Meyer) and ginsenoside Rg5

Shin-Jung Kim, An Keun Kim*

College of Pharmacy, Sookmyung Women's University, Seoul, Korea

ARTICLE INFO

Article history:
Received 8 July 2014
Received in Revised form
21 September 2014
Accepted 22 September 2014
Available online 18 October 2014

Keywords:
anticancer
breast cancer
cell cycle arrest
Fine Black ginseng (*Panax ginseng* Meyer)
ginsenoside Rg5

ABSTRACT

Background: Black ginseng (*Ginseng Radix nigra*, BG) refers to the ginseng steamed for nine times and fine roots (hairy roots) of that is called fine black ginseng (FBG). It is known that the content of saponin of FBG is higher than that of BG. Therefore, in this study, we examined antitumor effects against MCF-7 breast cancer cells to target the FBG extract and its main component, ginsenoside Rg5 (Rg5).
Methods: Action mechanism was determined by MTT assay, cell cycle assay and western blot analysis.
Results: The results from MTT assay showed that MCF-7 cell proliferation was inhibited by Rg5 treatment for 24, 48 and 72 h in a dose-dependent manner. Rg5 at different concentrations (0, 25, 50 and 100 μM), induced cell cycle arrest in G0/G1 phase through regulation of cell cycle-related proteins in MCF-7 cells. As shown in the results from western blot analysis, Rg5 increased expression of p53, $p21^{WAF1/CIP1}$ and $p15^{INK4B}$ and decreased expression of Cyclin D1, Cyclin E2 and CDK4. Expression of apoptosis–related proteins including Bax, PARP and Cytochrome c was also regulated by Rg5. These results indicate that Rg5 stimulated cell apoptosis and cell cycle arrest at G0/G1 phase via regulation of cell cycle-associated proteins in MCF-7 cells.
Conclusion: Rg5 promotes breast cancer cell apoptosis in a multi-path manner with higher potency compared to 20(S)-ginsenoside Rg3 (Rg3) in MCF-7 (HER2−/ER+) and MDA-MB-453 (HER2+/ER−) human breast cancer cell lines, and this suggests that Rg5 might be an effective natural new material in improving breast cancer.

1. Introduction

Ginseng (*Panax ginseng* Meyer) is a well characterized medicinal herb listed in the classic oriental herbal dictionary, *Shin-nong-bon-cho-kyung*. Ginseng has a sweet taste, is able to keep the body warm, and has protective effects on the five viscera (i.e., heart, lung, liver, kidney, and spleen) [1]. Ginseng can be classified by how it is processed. Red ginseng (RG; Ginseng Radix Rubra) refers to ginseng that has been steamed once. White ginseng (Ginseng Radix Alba) refers to dried ginseng. Black ginseng (BG; Ginseng Radix Nigra) is produced by repeatedly steaming fresh ginseng nine times. The fine roots (hairy roots or fibrous roots) of fresh ginseng that has been steamed nine times are called Fine Black ginseng (FBG). There are more than 30 different ginseng saponins with various physiological and pharmacological activities [2,3]. Ginsenosides are divided into two groups: protopanaxadiols and protopanaxatriols.

The root of *Panax ginseng* reportedly has various biological effects, including anticarcinogenic effects. One study showed that ginseng extracts induce apoptosis and decrease telomerase activity and cyclooxygenase-2 (COX-2) expression in human leukemia cells [4]. In addition, ginseng extracts suppress 1,2-dimethylhydrazine-induced colon carcinogenesis by inhibiting cell proliferation [5].

Until recently, research on anticancer effects of ginseng has focused on ginsenoside Rg3 (Rg3) and ginsenoside Rh2 (Rh2). Ginsenoside Rg3 is not present in raw ginseng or White ginseng, but is synthesized during heating hydrolysis; thus, only a small amount of Rg3 is present in Red ginseng. Ginsenoside Rg3 has an anticancer effect by suppressing phorbol ester-induced COX-2 expression and decreasing activation of nuclear factor kappa-light-chain-enhancer of activated B cells (NF-κB) [6]. Its blood pressure lowering effects have been identified in rat aorta through enhancing endothelium-dependent relaxation [7]. Ginsenoside Rg3 in methanol extraction of heat-processed ginseng has antioxidative and antitumor effects [8].

Ginsenoside Rh2 is a major active anticancer saponin in ginseng extracts [9]. Ginsenoside Rh2 treatment modulates the protein expression level of p21 and cyclin D, and leads to a marked reduction in the proliferation of MCF-7 human breast cancer cells

* Corresponding author. Sookmyung Women's University, Cheongpa-ro 47-gil 100, Youngsan-gu, Seoul, 140-742, Korea.
E-mail address: akkim@sookmyung.ac.kr (A.K. Kim).

1226-8453/$ – see front matter
http://dx.doi.org/10.1016/j.jgr.2014.09.003

[10]. It also provokes apoptosis through activating p53 and inducing the proapoptotic regulator Bax in colorectal cancer cells [11]. In addition, Rh2 markedly reduces the viability of breast cancer cells (MCF-7 and MDA-MB-231) by arresting the G1 phase cell cycle *via* p15 ^{INK4B} and p27 ^{KIP1}-dependent inhibition of cyclin-dependent kinases [12].

Many studies on BG have been performed because interest in it has increased recently. The main component of BG is reportedly Rg5 (Fig. 1) [13]. Studies demonstrate it has diverse physiological activity such as anti-inflammatory effects on lipopolysaccharide-stimulated BV2 microglial cells [14], protective effects on scopolamine-induced memory deficits in mice [15], and inhibitory effects in a mouse model with oxazolone-induced chronic dermatitis [16]. Rg5 reportedly blocks the cell cycle of SK-HEP-1 cells at the Gl/S transition phase by downregulating cyclin E-dependent kinase activity [17].

Breast cancer is a very common cancer in women worldwide. In the United States, it is estimated that breast cancer is the leading cause of all cancers (29%) and the second leading cause of death (14%) [18]. In Korea, 16,015 new cases of breast cancer were reported in 2011 [19]. Anticancer activity of BG extract in the MCF-1 breast cancer cell line exhibited three-fold cytotoxicity, compared with Red ginseng extract [20]. However, ginseng fine roots contain a higher content of ginseng saponin than ginseng main roots [2]. In the present study, we therefore aimed to investigate anti-breast cancer activity (in the MCF-7 cell line) and the action mechanisms of FBG ethanol extract (EE), FBG butanol fraction (BF; primarily containing saponin), and Rg5 as the major saponin.

2. Materials and methods

2.1. Materials

Fine Black ginseng (*Panax ginseng* Meyer) for experiments was purchased from Kumsan Town, Chungcheongnam Province, the Republic of Korea in August 2009. All other chemicals were of an analytical reagent grade. Distilled water for high-performance liquid chromatography (HPLC) and acetonitrile were purchased from J.T. Baker SOLUSORB (Philipsburg, NJ, USA). The standards were purchased from Chromadex (Santa Ana, CA, USA) and Ambo Institute (Seoul, South Korea). Proton magnetic resonance, carbon magnetic resonance, heteronuclear multiple quantum coherence and heteronuclear multiple bond coherence spectra were measured with INOVA-500 (500 MHz) (Varian, palo alto, CA, USA).

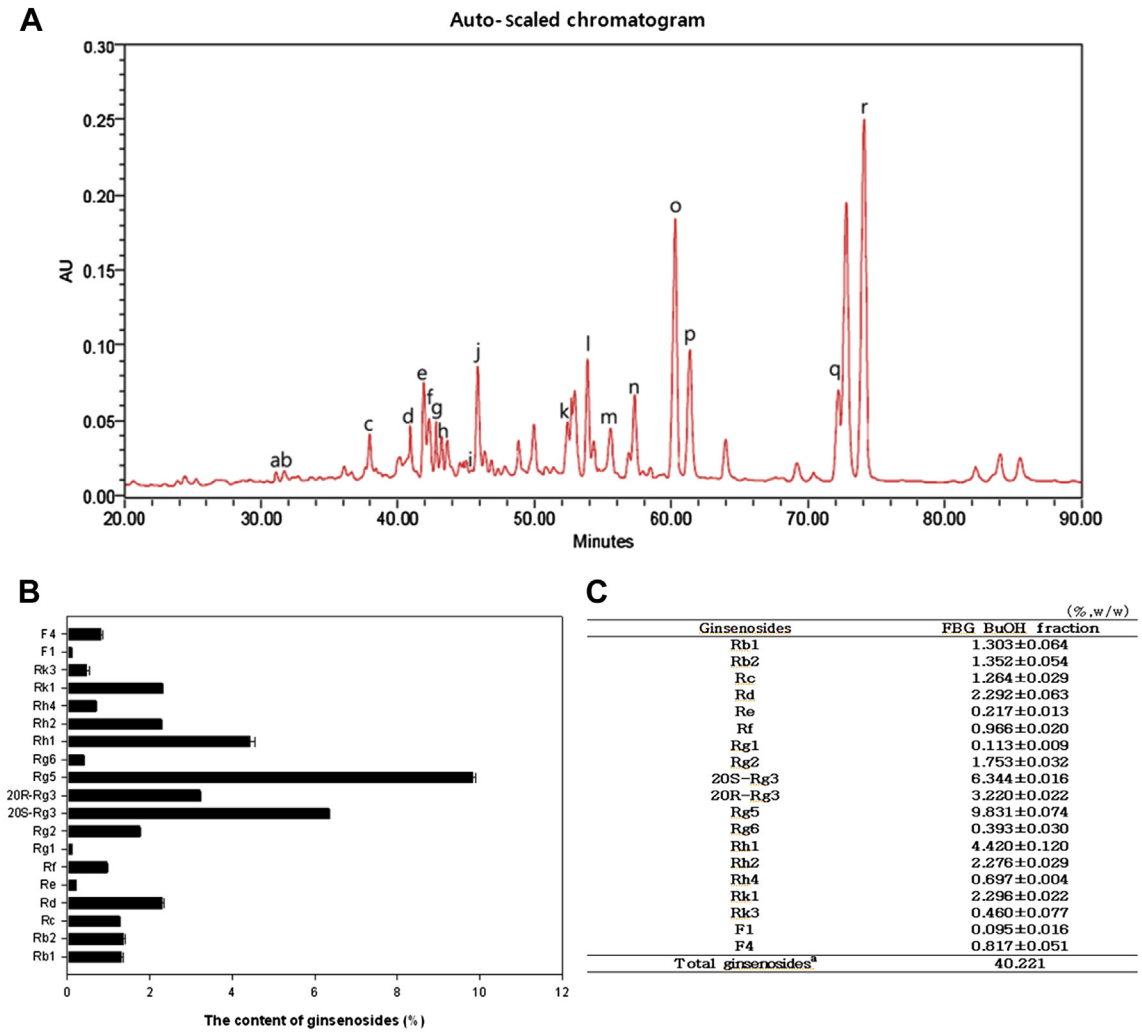

Fig. 1. (A) High-performance liquid chromatography chromatogram of ginsenosides in the butanol (BuOH) fraction of Fine Black ginseng (FBG), compared with the chromatogram of the ginsenoside standards: a, Rg1; b, Re; c, Rf; d, Rb1; e, Rg2; f, Rh1; g, Rc; h, Rb2; i, F1; j, Rd; k, Rg6; l, F4; m, Rk3; n, Rh4; o, (20S) Rg3; p, (20R) Rg3; q, Rk1; r, Rg5. (B) The content of ginsenosides and (C) the composition of ginsenosides in BuOH fraction of Fine Black ginseng.

The mass spectrum was taken on a fast atom bombardment mass spectrometry device (JMS-700; Jeol, Seoul, Korea). For the experiments, Rg3 was purchased from Chromadex. Rosewell Park Memorial Institute (RPMI 1640) medium (Buffalo, NY, USA), fetal bovine serum (FBS), trypsin-EDTA, and penicillin/streptomycin were purchased from Welgene (Daegu, South Korea); and (3-(4,5-dimethyl-2-thiazolyl)-2,5-diphenyl-2H-tetrazolium bromide (MTT) and 3,3′-dihexyloxacarbo-cyanine iodide ($DiOC_6$) were purchased from Sigma-Aldrich (St. Louis, MO, USA). The following antibodies were used: poly (ADP-ribose) polymerase (PARP), Bid, DR5, caspase-8, cleaved caspase-7, cleaved caspase-6, p53, β-actin (Cell signaling, Danvers, MA, USA); cytochrome C (BD Biosciences, San Jose, CA, USA); and Bcl-2, Bax, and DR4 (Santa Cruz Biotechnologies, Santa Cruz, CA, USA).

2.2. Preparation of ethanol extract and butanol fraction

Fine Black ginseng (10 kg) was selected, dried, and powdered. Exactly 2 kg of powdered samples were refluxed two times with 10 L of 95% ethyl alcohol for 2 h in a water bath. The extracts were filtered through filter paper (Nylon membrane filters 7404-004; Whatman, Dassel, Germany) and concentrated by a vacuum evaporator (yield: 18.35%). Ethyl alcohol extract (150 g) was dissolved in 1500 mL of water and extracted with 1500 mL of diethyl ether. The aqueous layer was extracted three times with 1500 mL of water-saturated *n*-butanol (n-BuOH). The n-BuOH fraction (84.50 g) was evaporated.

2.3. HPLC analysis

The ginsenoside composition of the concentrate was analyzed by HPLC, as suggested by Ko and colleagues [13,21]. The total ginsenoside content and composition of each sample were analyzed three times. The 99% pure ginsenoside standards used in this experiment were purchased from Chromadex and the Ambo Institute. For the experiment, the Waters 1525 binary HPLC system (Waters, Milford, MA, USA) and the Eurospher 100-5 C 18 column (3 × 250 mm; Knauer, Berlin, Germany) were used. The mobile phase was a mixture of acetonitrile (HPLC grade) and distilled water (HPLC grade). The content of acetonitrile was sequentially increased from 17% to 30% (35 min), from 30% to 40% (60 min), from 40% to 60% (100 min), from 60% to 80% (110 min), from 80% to 80% (120 min), from 80% to 100% (125 min), from 100% to 100% (135 min), and finally from 100% back to 17% (140 min, lasting for 5 min). The operating temperature was at room temperature and the flow rate was 0.8 mL/min. The elution profile on the chromatogram was obtained by using a UV/VIS detector at 203 nm (Waters 2487 dual λ absorbance detector; Waters) (Fig. 1A).

2.4. Isolation and identification of ginsenoside Rg5

The n-BuOH fraction (60 g) was chromatographed on a silica gel column (1 kg) with eluting solvents of $CHCl_3$-MeOH-H_2O (70:30:4) to obtain six subfractions (F1–F5). The F4 fraction (2.59 g) was further subjected to octadecylsilane (ODS) (C-18) column chromatography (500 g, 60% acetonitrile (ACN)) to provide Rg5 (0.19 g) (Fig. 1B).

In the FAB-MS spectrum of compound I $[M-H]^-$ peak appeared at m/z 765. ^{1}H-NMR spectrum (pyridine-d_5) showed eight methyl signals (CH3-18, 30, 29, 19, 28, 27, 26, 21) at δ 0.835, 0.979, 1.040, 1.130, 1.313, 1.603, 1.644, 1.840, H-3 and H-23 signals at δ 3.288, δ 2.791, On the other hand, proton signal resulting from the binding to C-3 glucose, and it was confirmed from δ 3.937 to δ 4.597. And the H-1′ and H-1″ signal from the binding to C-3 glucose was confirmed in δ 4.950 and δ 5.400. ^{13}C-NMR spectrum (pyridine-d_5) showed C-1, C-2, C-3, C-4, C-5, C-6, C-7, C-8, C-9, C-10, C-11, C-12, C-13, C-14, C-15, C-16, C-17, C-18, C-19, C-20, C-21, C-22, C-23, C-24, C-25, C-26, C-27, C-28, C-29, C-30, 3-Glc C-1′, 3-Glc C-2′, 3-Glc C-3′, 3-Glc C-4′, 3-Glc C-5′, 3-Glc C-6′, 3-Glc C-1″, 3-Glc C-2″, 3-Glc C-3″, 3-Glc C-4″, 3-Glc C-5″, 3-Glc C-6″ signals at δ 39.76, 28.60, 89.42, 40.75, 56.89, 18.93, 35.84, 40.21, 51.26, 37.51, 32.72, 73.08, 50.94, 51.52, 33.13, 27.25, 51.40, 16.94, 17.09, 140.66, 13.66, 123.82, 27.95, 123.92, 131.74, 26.18, 18.22, 28.60, 16.31, 17.52, 105.62, 83.95, 78.45, 72.15, 78.76, 63.34, 106.55, 77.64, 78.84, 72.12, 78.62, 63.19 (Fig. 2) [22].

2.5. Cell culture and MTT assay

MCF-7 (HER2-/ER+) and MDA-MB-453 (HER2+/ER−) human breast cancer cell lines were maintained using RPMI 1640 medium supplemented with 10% (vol/vol) FBS (Welgene, Daegu, South Korea) plus 100 units/mL penicillin and streptomycin in a 5% carbon dioxide air incubator at 37°C. Cell cytotoxicity was measured by MTT assay. Cells were seeded in 96-well tissue culture plates at the density of 0.2 × 10^4 cells per well with 100 μL medium, and were allowed to become attached for 24 h. One hundred microliters of the medium with different concentrations of Rg5 (e.g., 0μM, 25μM, 50μM, and 100μM) were added to each well. At indicated times, 30 μL MTT stock solution (3 mg/mL) were added to each well. After culturing the cells at 37°C for 2 h, dimethyl sulfoxide (DMSO) was added to dissolve the formazan crystals. The absorbance was read at the wavelength of 540 nm with a microplate reader (EL800, Biotek Instruments Inc., Winooski, VT, USA).

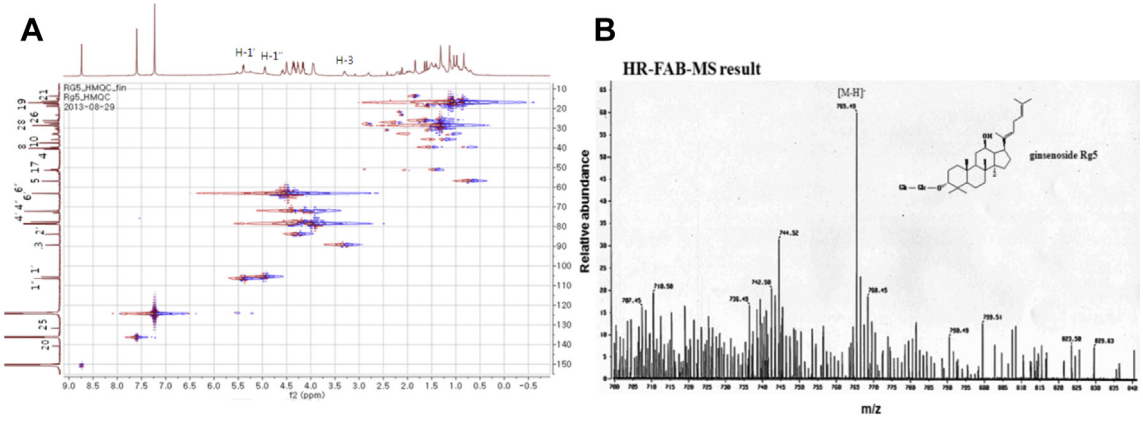

Fig. 2. (A) The HMQC (500 MHz, in pyridine) and (B) the fast atom bombardment mass spectroscopy spectrum of ginsenoside Rg5.

2.6. Western blot analysis

After treatment, the pellet of cells was rinsed with ice-cold phosphate buffered saline (PBS) and lysed in radioimmunoprecipitation assay buffer (0.1% sodium dodecyl sulfate, 0.5% sodium deoxycholate, 50mM Tris-HCl and 0.1% NP-40, pH 8.0 with 150mM sodium chloride) for 1 h at 4°C. The cell lysate was cleared by centrifugation at 17,000 rpm for 10 min at 4°C. Each supernatant sample was separated by 10% sodium dodecyl sulfate–polyacrylamide gel electrophoresis and the separated protein was transferred to polyvinylidene fluoride (PVDF) membranes. After blocking with 5% nonfat dry milk in TBS-T (25mM Tris and 0.1% Tween 20, 137mM sodium chloride) at room temperature (RT) for 2 h, the membranes were incubated with primary antibodies overnight at 4°C and treated with horseradish peroxidase-conjugated secondary antibodies for 2 h. The signals were detected with the ECL Advance Detection Kit (GE Healthcare Bio-Sciences Corp., Piscataway, NJ, USA) by LAS-3000 luminescent image analysis.

2.7. Annexin V/fluorescein isothiocyanate/propidium iodide assay and analysis of surface expression of DR4 and DR5

Apoptosis was evaluated by annexin V/fluorescein isothiocyanate/propidium iodide (annexin V-FITC/PI) dual staining. Treated

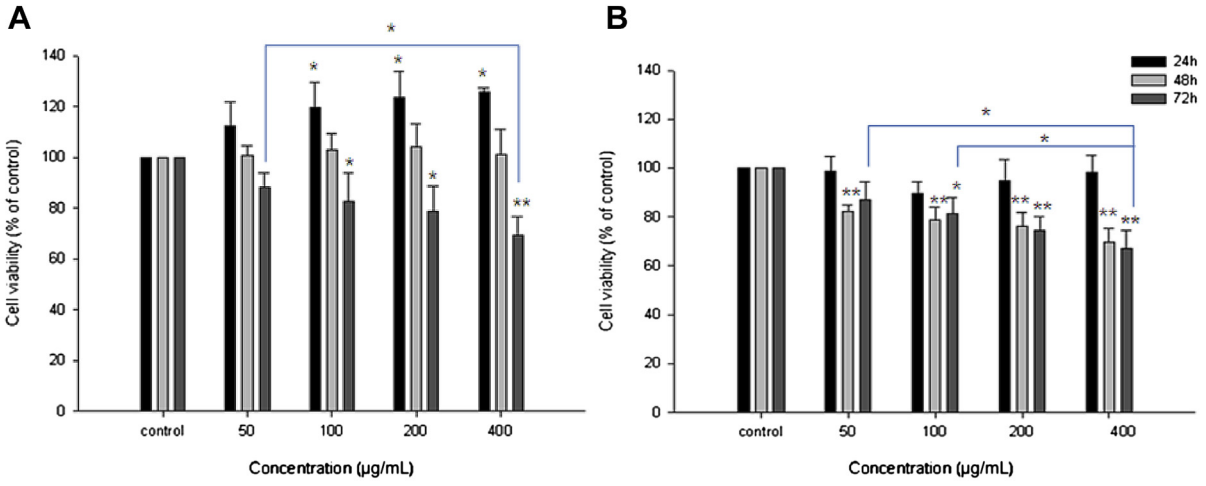

EE(453)	24h	48h	72h
50 μg/mL	112.48±9.22	101.76±2.26	100.05±6.59
100 μg/mL	119.67±9.7	104.06±5.09	100.88±3.3
200 μg/mL	123.75±9.99	106.27±9.8	111.73±1.31
400 μg/mL	125.78±1.81	103.67±10.65	111.01±6.54

EE(MCF-7)	24h	48h	72h
50 μg/mL	98.71±6.05	82.30±2.66	86.89±7.50
100 μg/mL	89.44±4.80	78.98±5.13	81.53±6.40
200 μg/mL	94.91±8.46	76.12±5.82	74.62±5.64
400 μg/mL	98.45±6.91	69.88±5.53	67.12±7.24

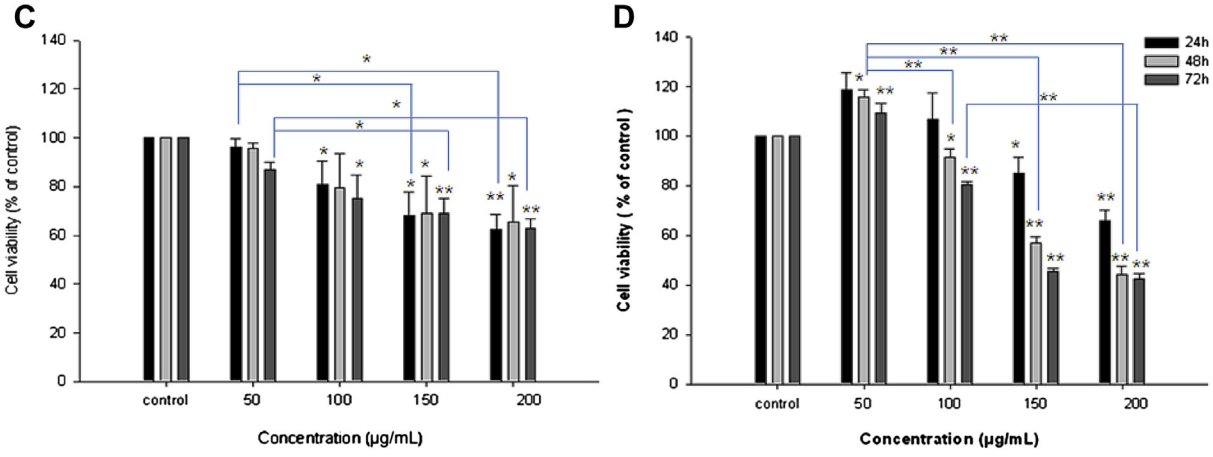

BF(453)	24h	48h	72h
50 μg/mL	95.96±3.49	95.86±2.17	86.82±3.14
100 μg/mL	80.59±9.69	79.61±14.03	75.29±9.43
150 μg/mL	68.05±9.67	68.99±15.12	68.87±6.42
200 μg/mL	62.5±6.27	65.42±14.96	63.01±4.03

BF(MCF-7)	24h	48h	72h
50 μg/mL	118.58±6.80	115.70±3.08	109.58±3.84
100 μg/mL	106.98±10.46	91.40±3.48	80.28±1.41
150 μg/mL	85.14±6.19	56.76±2.66	45.56±1.15
200 μg/mL	65.14±4.45	44.27±3.32	42.46±2.11

Fig. 3. (A and B) Effects of ethanol extraction and (C and D) BF of FBG on cell viability in MDA-MB-453 [453] (HER2+/ER−) and MCF-7 (HER2−/ER+) breast cancer cell lines. Cells were seeded in the 96-well plate at 2×10^3 cells per well and treated as indicated. Cell viability was evaluated by 3-(4,5-dimethyl-2-thiazolyl)-2,5-diphenyl-2H-tetrazolium bromide (MTT) assay. Statistical significance at $^*p < 0.05$ and $^{**}p < 0.001$, versus the control. EE, ethanol extract; BF, butanol fraction; FBG, Fine Black ginseng.

cells were harvested and resuspended in 1× binding buffer. A combination of annexin V/FITC solution and PI solution were added to each tube. The stained cells were incubated at room temperature for 30 min in the dark. Samples were analyzed by the FACSCanto II Flow Cytometer (BD Biosciences, San Jose, CA, USA).

Cells were analyzed for their cell surface expression of DR4 and DR5 by indirect staining with primary mouse anti-human DR4 and DR5, followed by phycoerythrin (PE)-conjugated goat anti-mouse immunoglobulin G_1 (IgG_1). The treated cells were harvested and washed with PBS containing 1% bovine serum albumin. Cells were incubated with anti-DR4 or anti-DR5 antibody for 30 min at 4°C in the dark. After incubation, cells were washed twice and reacted with PE-labeled secondary antibody for 30 min at 4°C in the dark. Isotype-matched nonbinding antibodies (Iso) were the negative control cells. Samples were measured by flow cytometry.

2.8. Analysis of cell cycle and microscopic images of DAPI staining

Analysis of the cell cycle was performed by staining with PI. Cells were seeded into a 100-mm dish, which contained 1×10^6 cells per plate. After 24 h, the media were changed to RPMI 1640 medium supplemented with indicated concentrations of Rg5. After 48 h of incubation, the cells were trypsinized and washed with ice-cold PBS, fixed with ice-cold 90% ethanol, and then incubated at −20°C until analysis. For cell cycle analysis, the cells were resuspended in 300 mL of PBS containing 30 μL RNase A solution (10 mg/mL; Sigma-Aldrich) and 1.5 μL PI solution (1 mg/mL; Molecular Probes). After incubation at 37°C for 30 min, cells were determined using the FACSCanto II Flow Cytometer (BD Biosciences, San jose, CA, USA). The cell cycle distribution was analyzed by FlowJo software (Tree Star, Inc., Ashland, OR, USA).

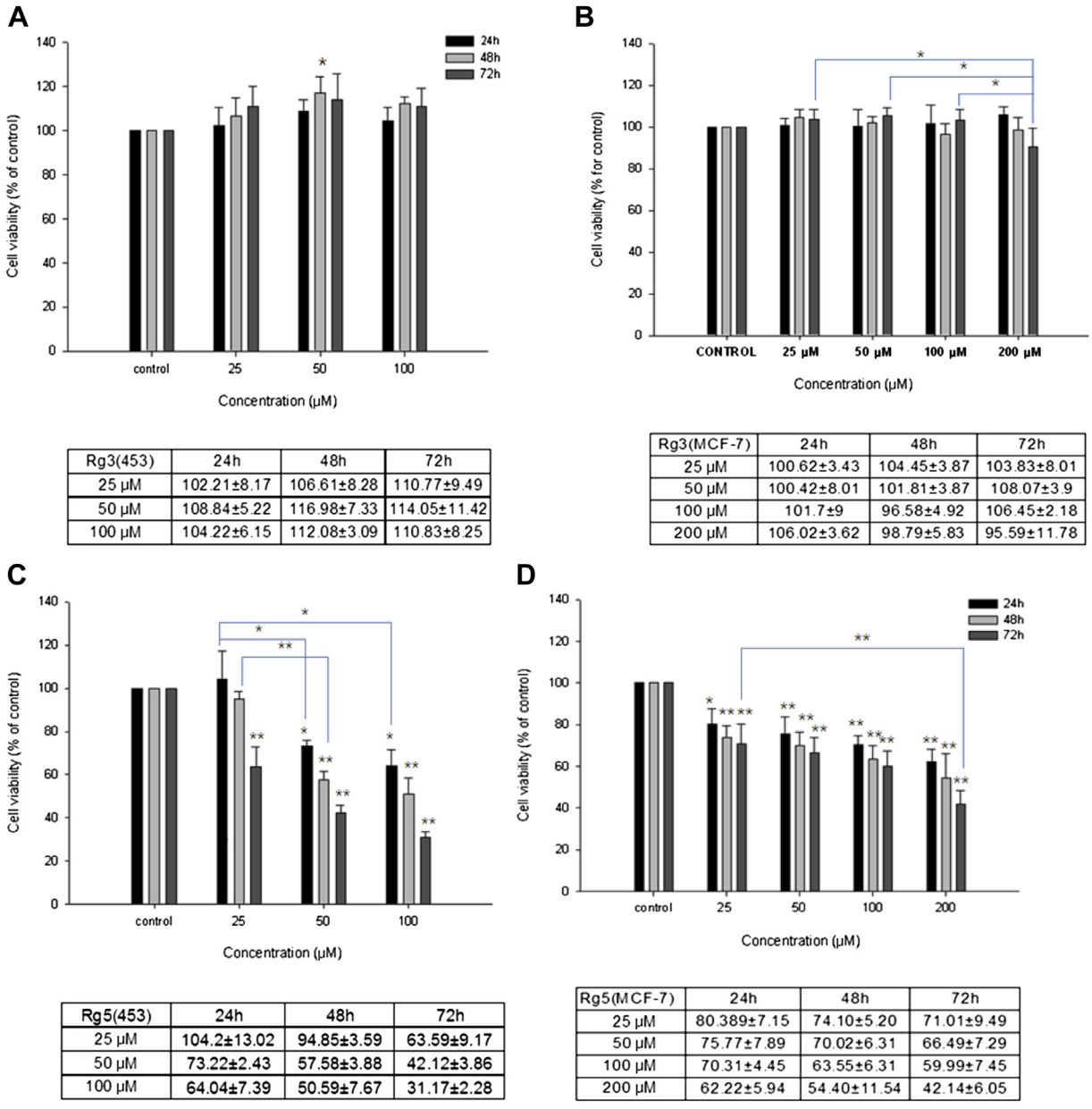

Rg3(453)	24h	48h	72h
25 μM	102.21±8.17	106.61±8.28	110.77±9.49
50 μM	108.84±5.22	116.98±7.33	114.05±11.42
100 μM	104.22±6.15	112.08±3.09	110.83±8.25

Rg3(MCF-7)	24h	48h	72h
25 μM	100.62±3.43	104.45±3.87	103.83±8.01
50 μM	100.42±8.01	101.81±3.87	108.07±3.9
100 μM	101.7±9	96.58±4.92	106.45±2.18
200 μM	106.02±3.62	98.79±5.83	95.59±11.78

Rg5(453)	24h	48h	72h
25 μM	104.2±13.02	94.85±3.59	63.59±9.17
50 μM	73.22±2.43	57.58±3.88	42.12±3.86
100 μM	64.04±7.39	50.59±7.67	31.17±2.28

Rg5(MCF-7)	24h	48h	72h
25 μM	80.389±7.15	74.10±5.20	71.01±9.49
50 μM	75.77±7.89	70.02±6.31	66.49±7.29
100 μM	70.31±4.45	63.55±6.31	59.99±7.45
200 μM	62.22±5.94	54.40±11.54	42.14±6.05

Fig. 4. The effects of the (A and B) ginsenoside Rg3 and (C and D) ginsenoside Rg5 on cell viability in MDA-MB-453 (HER2+/ER−) and MCF-7 (HER2−/ER+) breast cancer cell lines. Cells were treated with the indicated concentration of ginsenosides for 24 h, 48 h, and 72 h. Cell viability was assessed by 3-(4,5-dimethyl-2-thiazolyl)-2,5-diphenyl-2H-tetrazolium bromide (MTT) assay. * Indicates a significant difference at $p < 0.05$, versus the control. ** Indicates a significant difference at $p < 0.001$, versus the control.

Cells were plated at 0.3 × 10^6 cells in six-well plates. After treatment, the cells were fixed in DMSO/methanol (1:4) solution for 12 h at 4°C, stained with 4′,6-diamidino-2-phenylindole (DAPI) for 20 min, and observed by fluorescence microscopy.

2.9. Statistical analysis

Statistical significance was performed by Turkey's multiple comparison tests (Sigma Plot version 10.0; Systat Software, San Jose, CA). All experiments were repeated at least three times. Data were analyzed by one-way analysis of variance (ANOVA), and each value was presented as the mean ± the standard deviation.

3. Results

3.1. Isolation and analysis of ginsenoside Rg5

The yield of ginsenosides from ginseng hairy root (i.e., fine root) was higher than the yield from the main root [2], and the saponin content of FBG was higher than that of BG [23]. First of all, the HPLC results showed Rg5 was the main constituent among the ginsenosides in FBG (Fig. 1A). Rg5 was separated from FBG BF using column chromatography (silica gel, ODS) (Figs. 1B, 1C), and the chemical structure was confirmed by spectroscopic methods [e.g., NMR, mass spectroscopy (MS)] (Fig. 2).

3.2. Cytotoxicity of the FBG extract and its main component, ginsenoside Rg5

The effects of FBG EE and FBG BF on cell viability were evaluated in MCF-7 and MDA-MB-453 breast cancer cell lines by MTT assay. The results showed that EE reduced MCF-7 cell viability after 48 h of treatment and it decreased cell viability of MDA-MB-453 cells after 72 h (Figs. 3A, 3B). Increased cell viability was detected in MCF-7 cells when it was treated with 50 μg/mL (at 24 h, 48 h, and 72 h) and 100 μg/mL (24 h) of BF, but at higher concentrations (150 μg/mL and 200 μg/mL) the cell viability was decreased in a dose-dependent manner (Figs. 3C, 3D). As Figs. 4C and 4D show, Rg5, the main component of FBG, exerted significant cytotoxicity in a dose- and time-dependent manner. The cytotoxic effect of 20(S)-Rg3 in MCF-7 cells unexpectedly showed no significant difference. These results were consistent when Rg3 was treated in MDA-MB-453 cells (Figs. 4A, 4B).

3.3. Effects of ginsenoside Rg5 on cell cycle arrest

The results from flow cytometric analysis [i.e., fluorescence-activated cell sorting (FACS)] indicated that Rg5 significantly induced cell cycle arrest (Figs. 5A, 5B). This was further confirmed by the cell cycle assay with the data representing suppressed cell proliferation in MCF-7 cells after Rg5 treatment. Rg5 increased the number of cells in the G0/G1 phase and decreased the number of cells in the S phase. Based on these results, Rg5 may induce cell cycle arrest at the G0/G1 phase. Protein expression of cyclin D1, cyclin E2 and CDK4 was decreased, whereas the expression of $p15^{INK4B}$, p53 and $p21^{WAF1/CIP1}$ was increased (Figs. 6A, 6B).

3.4. Effects of ginsenoside Rg5 on apoptosis-related proteins

As Fig. 7A shows, treatment with Rg5 induced caspase-8 and caspase-9, caspase-7, caspase-6. The full-length Bid consequently disappeared in a dose-dependent manner. Poly (ADP-ribose) polymerase (PARP) cleavage was detected in Rg5-treated MCF-7 cells, which indicated that Rg5 reduced cell viability by inducing apoptosis. Promotion of mitochondria-mediated intrinsic apoptotic pathway by Rg5 was evidenced by Bax/Bcl-2 dysregulation,

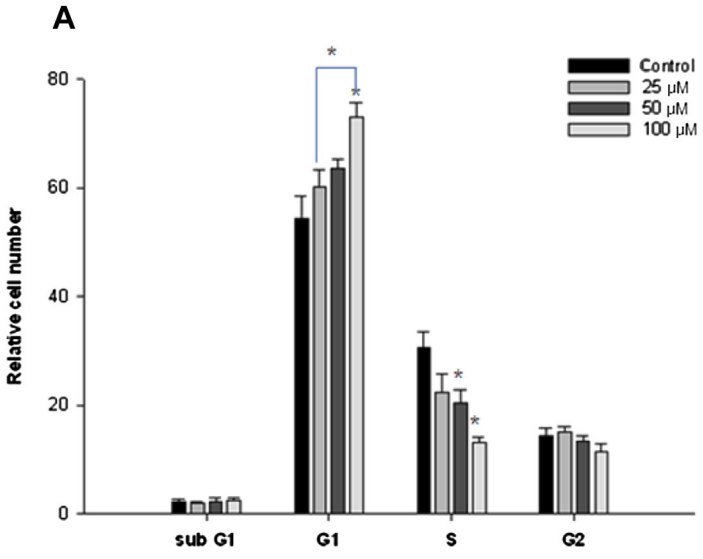

Rg5(MCF-7)	sub G1	G1	S	G2
Control	2.44±0.46	54.48±4.15	30.73±2.96	14.47±1.37
25 μM	2.05±0.22	60.25±3.22	22.53±3.25	15.1±1.14
50 μM	2.21±0.88	63.55±1.66	20.06±2.42	13.55±0.79
100 μM	2.46±0.69	73.03±2.67	13.2±1.04	11.63±1.24

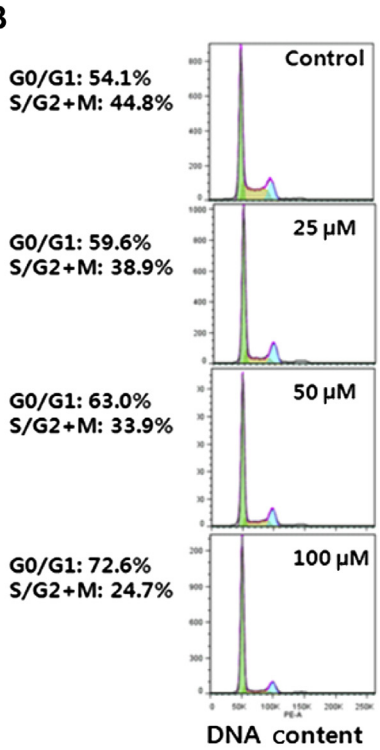

Fig. 5. The effect of ginsenoside Rg5 on cell cycle arrest at the G0/G1 phase. Cells were treated with dimethyl sulfoxide (0.01%) or ginsenoside Rg5 (25μM, 50μM, and 100μM) for 48 h. The cell cycle was measured by fluorescence-activated cell sorting. The data are representative of at least three independent experiments. * Indicates a significant difference at $p < 0.001$, versus the control.

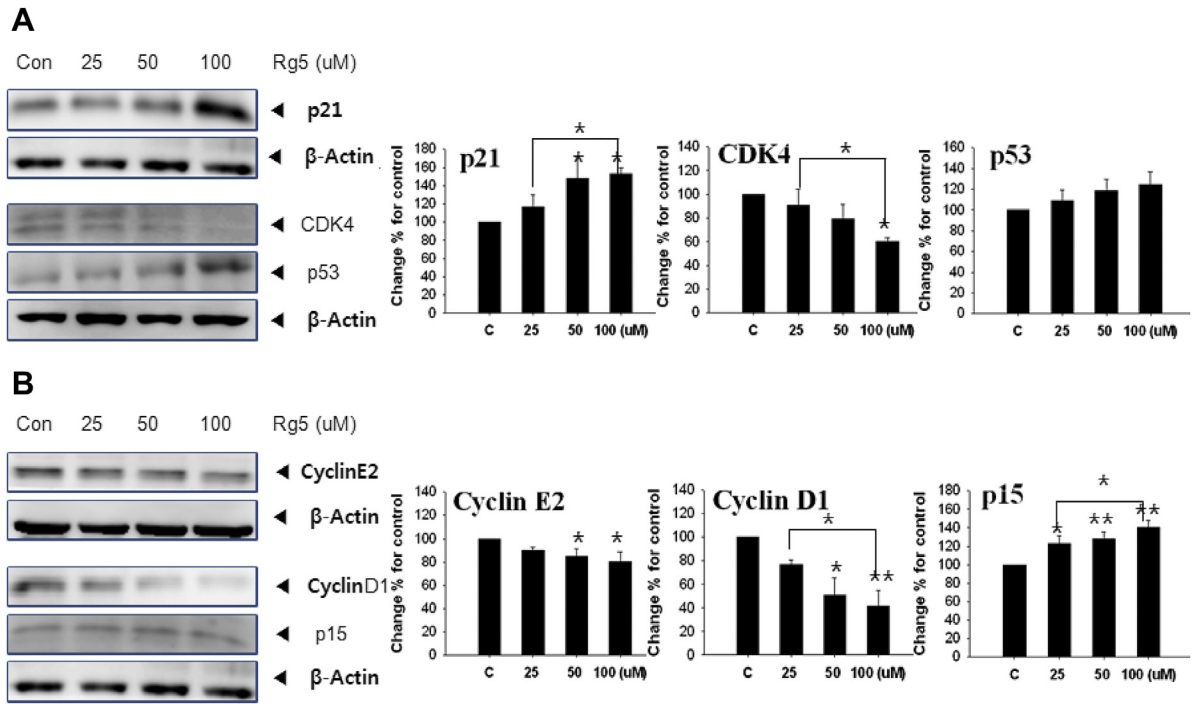

Fig. 6. Effects of ginsenoside Rg5 on G1-related proteins in MCF-7 cells. Cells were treated with DMSO (0.01%) or ginsenoside Rg5 (25, 50 and 100 μM) for 48 h. Protein expressions were determined using western blotting. $^{*}p < 0.05$, $^{**}p < 0.001$ versus control are significant different.

activation of caspase-9, and release of cytochrome C (Fig. 7A). Apoptosis was evaluated by annexin V/FITC/PI dual staining. After 48 h, Rg5 significantly increased apoptosis at 25μM and 50μM and reduced apoptotic cells at 100μM, whereas necrotic cells were increased (Fig. 7B). The increased expression of DR4 and DR5 on the cell surface was obvious when cells were treated at the 100μM concentration of Rg5 (Fig. 8A). Activation of p38 mitogen-activated protein kinases (MAPKs) is necessary for apoptosis induced by exposure to ultraviolet radiation, cytokines, chemotherapy, ceramide, and serum deprivation [24]. When cells were treated with Rg5 (50μM and 100μM), p38 MAPKs were activated with the generation of reactive oxygen species (data not shown) (Fig. 8C). Survivin, an inhibitor of apoptotic proteins, is highly expressed in most types of cancer and is a regulator of mitosis; survivin-targeting cancer treatment is validated with great efficacy and no serious toxicity [25]. The expression of survivin was suppressed at high

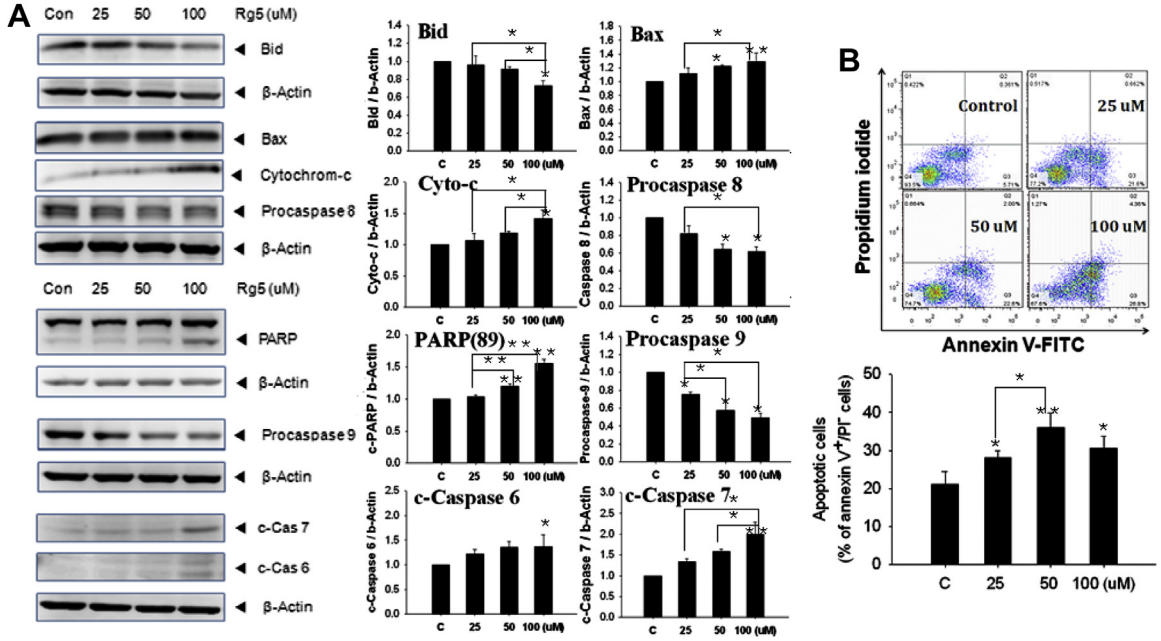

Fig. 7. Effects of ginsenoside Rg5 on MCF-7 cell apoptosis. (A) Effects of ginsenoside Rg5 on apoptosis-related proteins in MCF-7 cells. Cells were treated with DMSO (0.01%) or ginsenoside Rg5 (25, 50 and 100 μM) for 48 h. (B) Apoptosis was evaluated by Annexin V-FITC/PI dual staining. The value represents mean ± SD ($n = 3$). Statistical significance at $^{*}p < 0.05$, $^{**}p < 0.001$.

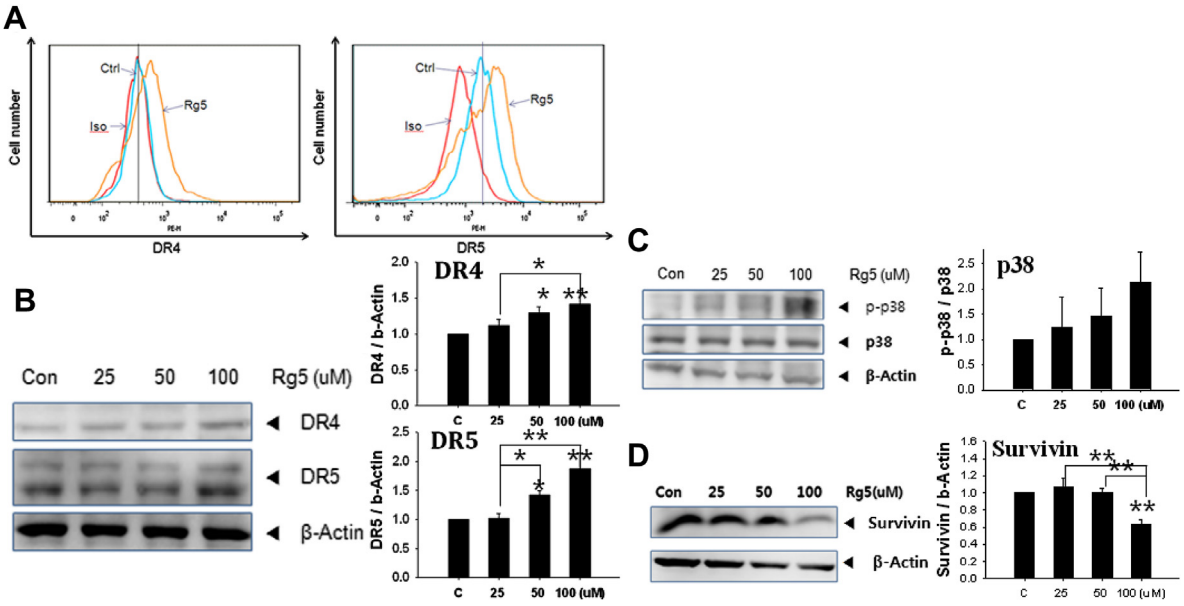

Fig. 8. (A) Effects of ginsenoside Rg5 on DR4 and DR5 expression in MCF-7 cells. The cells were incubated for 48 h with 100 μg/mL ginsenoside Rg5. DR4 and DR5 surface expressions were analyzed by FACS using PE-conjugated anti-DR4 and anti-DR5 antibodies. Isotype-matched nonbinding antibodies (Iso) were used as control for unspecific binding. (B) The protein levels of DR4 and DR5 were evaluated by western blotting. (C–D) The protein levels of p-p38/p38 and survivin were analyzed by western blotting. The bar represents the mean ± SD ($n = 3$). $^{*}p < 0.05$, $^{**}p < 0.001$ versus control are significantly different.

concentrations of Rg5 (Fig. 8D). Apoptotic cells were visualized with DAPI as fluorescent probes. When cells were incubated for 48 h with Rg5 at indicated concentrations (i.e., 0μM, 50μM, and 100μM), the cells displayed the typical apoptosis morphology such as fragmented and condensed nuclei with cellular shrinkage (Fig. 9B). Cells treated with Rg5 at the 100μM concentration showed a necrosis-like morphology (Fig. 9C).

4. Discussion

Red ginseng is fresh ginseng that is dry-steamed once using water vapor. Black ginseng refers to ginseng that is steamed nine times. Fine Black ginseng refers to the fine roots (i.e., hairy roots) of BG steamed nine times.

As Fig. 1C shows, FBG BF contained more than 40% of the total saponins. The amount of total saponin in the FBG BF was 17 times higher than in BG EE, and was 26 times higher than in RG EE [26]. Fine Black ginseng contained the highest content of Rg5 (9.831%) (Fig. 1C). The amount of Rg5 in FBG BF was 34 times higher than in BG EE, and was 110 times higher than in RG EE [26]. Rg5, the main component of FBG BF, was isolated using column (silica gel, ODS) chromatography, and the chemical structure was confirmed by spectroscopic analysis (i.e., NMR, MS) (Fig. 2).

The difference in chemical structure between Rg5 and Rg3 is the polar hydroxyl group of C-20 in Rg3. When C-20 is induced

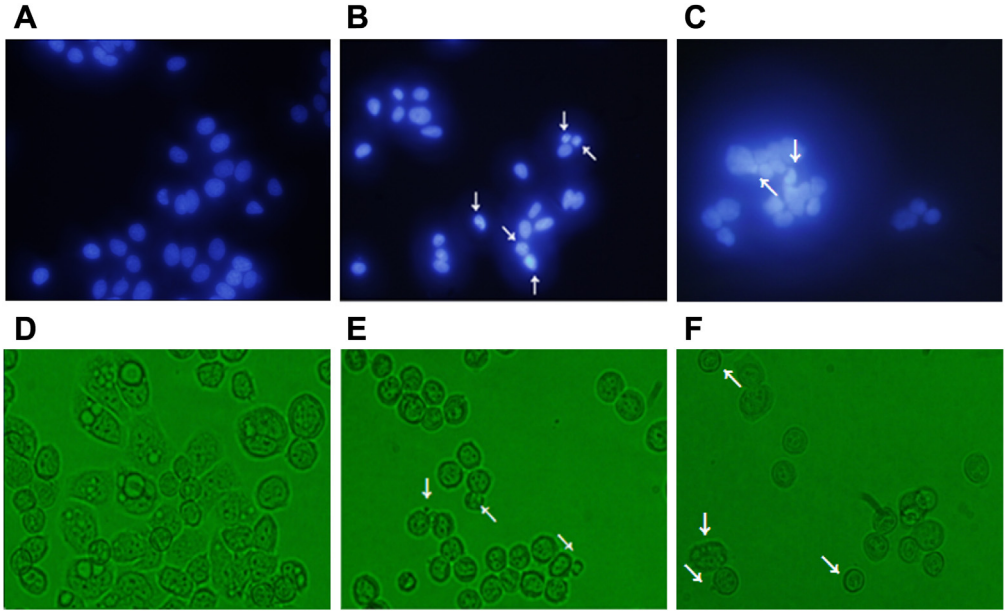

Fig. 9. Effects of ginsenoside Rg5 on MCF-7 cells (A, B, C) and MDA-MB-453 cells (D, E, F) morphology. Cells were treated with 50 and 100 μM ginsenoside Rg5 for 48 h and cell morphology was investigated under the fluorescence microscope. A, D: control (DMSO 0.01%), B, E: ginsenoside Rg5 50 μM, C, F: ginsenoside Rg5 100 μM.

dehydration reaction [43], that is applied to the high-pressure steam, Rg3 is converted to Rk1 and Rg5. Dehydration of the C-20 of the ginsenoside structure increases its bioactivity [27]. Rg5 (i.e., Rg3 that has been dehydrated at C-20) reportedly has cytostatic activity of human hepatoma SK-HEP-1 cells that is approximately four times stronger than that of Rg3 [17].

Therefore, the purpose of this study was to elucidate anti-breast cancer activity of FBG extract and Rg5 in MCF-7 cells. The FBG extract and Rg5 showed significant cytotoxic activity. In previous studies, the BG extract in comparison to RG extract exhibited stronger cytotoxic activity *in vitro* on the MCF-1 breast cancer cell line, HT-1080 fibrosarcoma cell line and Hepa1C1C7 murine hepatoma cell line [20].

The anticancer properties of Rg3 are associated with inducing apoptosis [28], regulating cell cycle [29], blocking angiogenesis [30], and inhibiting proliferation. Rg3 exhibits anticancer activity in various cell lines such as human hepatocellular carcinoma cells (Hep3B) [31], the PC-3M prostate cancer cell line [32], VX2 liver tumors [33], and the U87MG human glioblastoma cell line [28]. However, the cytotoxic effect of 20(S)-Rg3 in MCF-7 cells showed no significant difference, and the results were consistent when MDA-MB-453 cells were treated by Rg3 (Figs. 4A, 4B).

Cell cycle arrest and western blot analysis were performed to determine the mechanism of action for the anticancer effects of Rg5. As a result, Rg5 induced significant G0/G1 cell cycle arrest. The results of western blot analysis showed increased Bax (i.e., proapoptotic regulator), caspase-6 and caspase-7 (i.e., effector caspases), DR4, and DR5. These results were evident even when Rh2 induced apoptosis in colorectal cancer cells through activation of p53 [34]. The tumor suppressor p53 induces cell self-destruction through the endogenous mitochondrial pathway and exogenous death receptor pathway. This is called p53-dependent apoptosis (i.e., p53-induced apoptosis). In particular, p53-dependent apoptosis is used to induce the expression of proapoptotic members. Bax also is expressed by the activation of p53 [35,36]. When the cells undergo DNA damage, p53 stops the cell cycle through p21 or it induces apoptosis. In response to cellular stress or DNA damage, p53 is stabilized by post-transcriptional modifications and the level of p53 increases [37]. Stabilization and activation of p53 is responsible for cellular antiproliferative mechanisms such as apoptosis, growth arrest, and cell senescence [38]. This study confirmed the influence of Rg5 on the activity of Bax and p53.

The data showed that the expression of DR4 and DR5 was upregulated by Rg5 in a dose-dependent manner. The tumor necrosis factor-related apoptosis-inducing ligand (TRAIL) is a promising agent for cancer treatment because it selectively induces apoptosis in various cancer cells, but not in normal cells [39]. Many tumor cells are resistant to TRAIL-induced apoptosis. Therefore, it is important to develop combination therapies to overcome this resistance [40]. Rg5 did not increase TRAIL-induced apoptosis, which suggests that Rg5 does not increase the susceptibility of TRAIL-resistant MCF-7 cells. Therefore, Rg5 was unsuitable for combination therapy.

To examine whether Rg5 reduced cell viability via apoptosis, cells were analyzed by using annexin V-FITC/PI staining assay. Rg5 at 0μM, 25μM, and 50μM concentrations increased apoptosis in a dose-dependent manner. However, at 100μM concentration of Rg5, apoptotic cells were reduced, whereas necrotic cells were increased. There are many natural substances similar to this situation. Procyanidin, a polyphenol compound with strong bioactivity and pharmacologic activity, exists widely in grape seeds, hawthorn, and pine bark. Procyanidin induces apoptosis and necrosis of prostate cancer cell line PC-3 in a mitochondrion-dependent manner. With extended procyanidin treatment, the apoptosis rate decreased, whereas the necrosis rate increased. This change was associated with cytotoxic properties that were related to alterations in cell membrane properties [41,42].

Rg5 induces cancer cell apoptosis in a multipath mechanism, and is therefore a promising candidate for antitumor drug development. The antitumor role of Rg5 would be useful in therapeutic approaches (e.g., in combination therapy with other cancer chemotherapy drugs). In this study, we elucidated the effects of Rg5 in MCF-7 and MDA-MB-453 human breast cancer cell lines, which demonstrated that Rg5 may be an effective chemotherapeutic agent for breast cancer. However, further studies are needed to identify the precise mechanism of Rg5. There is also a need for *in vivo* experiments to confirm the anticancer activity of Rg5.

Conflicts of interest

The authors have no conflicts of interest to declare.

Acknowledgments

This research was supported by the Sookmyung Women's University Research Grants 1-1103-0741.

References

[1] Namba T. The encyclopedia of Wakan-Yaku with color pictures. Osaka: Hoikusha; 1980.
[2] Park JD. Recent studies on the chemical constituents of Korean Ginseng (*Panax ginseng* C.A. Meyer). Korea J Ginseng Sci 1996;20:389–415.
[3] Yokozawa T, Kobayashi T, Oura H, Kawashima Y. Studies on the mechanism of the hypoglycemic activity of ginsenoside-Rb2 in streptozotocin-diabetic rats. Chem Pharm Bull (Tokyo) 1985;33:869–72.
[4] Park SE, Park C, Kim SH, Hossain MA, Kim MY, Chung HY, Son WS, Kim GY, Choi YH, Kim ND. Korean Red Ginseng extract induces apoptosis and decreases telomerase activity in human leukemia cells. J Ethnopharmacol 2009;121:304–12.
[5] Fukushima S, WanibuchiH LW. Inhibition by ginseng of colon carcinogenesis in rats. J Korean Med Sci 2001;16:75–80.
[6] Keum YS, Han SS, Chun KS, Park KK, Park JH, Lee SK, Surh YJ. Inhibitory effects of the ginsenoside Rg3 on phorbol ester-induced cyclooxygenase-2 expression, NF-kappaB activation and tumor promotion. Mutat Res 2003;523–524:75–85.
[7] Kim ND, Kang SY, Park JH, Schini-Kerth VB. Ginsenoside Rg3 mediates endothelium-dependent relaxation in response to ginsenosides in rat aorta: role of K+ channels. Eur J Pharmacol 1999;367:41–9.
[8] Keum YS, Park KK, Lee JM, Chun KS, Park JH, Lee SK, Kwon H, Surh YJ. Antioxidant and anti-tumor promoting activities of the methanol extract of heat-processed ginseng. Cancer Lett 2000;150:41–8.
[9] Helms S. Cancer prevention and therapeutics: *Panax ginseng*. Altern Med Rev 2004;9:259–74.
[10] Oh M, Choi YH, Choi S, Chung H, Kim K, Kim SI, Kim DK, Kim ND. Antiproliferating effects of ginsenoside Rh2 on MCF-7 human breast cancer cells. Int J Oncol 1999;14:869–75.
[11] Li B, Zhao J, Wang CZ, Searle J, He TC, Yuan CS, Du W. Ginsenoside Rh2 induces apoptosis and paraptosis-like cell death in colorectal cancer cells through activation of p53. Cancer Lett 2011;301:185–92.
[12] Choi S, Kim TW, Singh SV. Ginsenoside Rh2-mediated G1 phase cell cycle arrest in human breast cancer cells is caused by p15 Ink4B and p27 Kip1-dependent inhibition of cyclin-dependent kinases. Pharm Res 2009;26:2280–8.
[13] Lee SA, Jo HK, Im BO, Kim S, Whang WK, Ko SK. Changes in the contents of prosapogenin in the Red Ginseng (*Panax ginseng*) depending on steaming batches. J Ginseng Res 2012;36:102–6.
[14] Lee YY, Park JS, Jung JS, Kim DH, Kim HS. Anti-inflammatory effect of ginsenoside Rg5 in lipopolysaccharide-stimulated BV2 microglial cells. Int J Mol Sci 2013;14:9820–33.
[15] Kim EJ, Jung IH, Van Le TK, Jeong JJ, Kim NJ, Kim DH. Ginsenosides Rg5 and Rh3 protect scopolamine-induced memory deficits in mice. J Ethnopharmacol 2013;146:294–9.
[16] Shin YW, Bae EA, Kim DH. Inhibitory effect of ginsenoside Rg5 and its metabolite ginsenoside Rh3 in an oxazolone-induced mouse chronic dermatitis model. Arch Pharm Res 2006;29:685–90.
[17] Lee KY, Lee YH, Kim SI, Park JH, Lee SK. Ginsenoside-Rg5 suppresses cyclin E-dependent protein kinase activity via up-regulating p21Cip/WAF1 and down-regulating cyclin E in SK-HEP-1 cells. Anticancer Res 1997;17:1067–72.
[18] Siegel R, Ma J, Zou Z, Jemal A. Cancer statistics, 2014. CA Cancer J Clin 2014;64:9–29.
[19] Statistics Korea. 2012 Annual report on the cause of death statistics. In: Office KNS, editor. Daejeon, Korea: Statistics Korea; 2013.

[20] Lee JH, Shen GN, Kim EK, Shin HJ, Myung CS, Oh HJ, Kim DH, Roh SS, Cho W, Seo YB, et al. Preparation of black ginseng and its antitumor activity. Korean J Oriental Physiol Pathol 2006;20:951–6.
[21] Ko SK, Bae HM, Cho OS, Im BO, Chung SH, Lee BY. Analysis of ginsenoside composition of ginseng berry and seed. Food Sci Biotechnol 2008;17:1379–82.
[22] Kim SI, Park JH, Ryu JH, Park JD, Lee YH, Kim TH, Baek NI. Ginsenoside Rg5, a genuine dammarane glycoside from Korean red ginseng. Arch Pharm Res 1996;19:551–3.
[23] Han ST, Whang WK, Kim IH, Yang BW, Cho SH, Ko SK. Analysis of ginsenosides of Black Ginseng. Yakhak Hoeji 2005;49:490–4.
[24] Benhar M, Dalyot I, Engelberg D, Levitzki A. Enhanced ROS production in oncogenically transformed cells potentiates c-Jun N-terminal kinase and p38 mitogen-activated protein kinase activation and sensitization to genotoxic stress. Mol Cell Biol 2001;21:6913–26.
[25] Fukuda S, Pelus LM. Survivin, a cancer target with an emerging role in normal adult tissues. Mol Cancer Ther 2006;5:1087–98.
[26] Jo HK, Sung MC, Ko SK. The comparison of ginseng prosapogenin composition and contents in Red and Black ginseng. Kor J Pharmacogn 2011;42:361–5.
[27] Kang KS, Kim HY, Yamabe N, Yokozawa T. Stereospecificity in hydroxyl radical scavenging activities of four ginsenosides produced by heat processing. Bioorg Med Chem Lett 2006;16:5028–31.
[28] Choi YJ, Lee HJ, Kang DW, Han IH, Choi BK, Cho WH. Ginsenoside Rg3 induces apoptosis in the U87MG human glioblastoma cell line through the MEK signaling pathway and reactive oxygen species. Oncol Rep 2013;30:1362–70.
[29] Song Y, Hou J, Kang L, Gao S. Effect of 20(S)-ginsenoside Rg3 on the proliferation inhibition and secretion of vascular endothelial growth factor of multiple myeloma cell line U266 [in Chinese]. Zhonghua Xue Ye Xue Za Zhi 2014;35:519–23.
[30] Kim JW, Jung SY, Kwon YH, Lee JH, Lee YM, Lee BY, Kwon SM. Ginsenoside Rg3 attenuates tumor angiogenesis via inhibiting bioactivities of endothelial progenitor cells. Cancer Biol Ther 2012;13:504–15.
[31] Park HM, Kim SJ, Kim JS, Kang HS. Reactive oxygen species mediated ginsenoside Rg3- and Rh2-induced apoptosis in hepatoma cells through mitochondrial signaling pathways. Food Chem Toxicol 2012;50:2736–41.
[32] Pan XY, Guo H, Han J, Hao F, An Y, Xu Y, Xiaokaiti Y, Pan Y, Li XJ. Ginsenoside Rg3 attenuates cell migration via inhibition of aquaporin 1 expression in PC-3M prostate cancer cells. Eur J Pharmacol 2012;683:27–34.
[33] Yu Y, Zhang C, Liu L, Li X. Hepatic arterial administration of ginsenoside Rg3 and transcatheter arterial embolization for the treatment of VX2 liver carcinomas. Exp Ther Med 2013;5:761–6.
[34] Guo XX, Li Y, Sun C, Jiang D, Lin YJ, Jin FX, Lee SK, Jin YH. p53-dependent Fas expression is critical for Ginsenoside Rh2 triggered caspase-8 activation in HeLa cells. Protein Cell 2014;5:224–34.
[35] Sheu MJ, Chou PY, Huang CS, Tsai IC, Chien YC, Lin SY, Tsai HY, Cheng HC, Wu CH. Pipoxolan inhibits proliferation of HL-60 human leukaemia cancer cells by arresting the cell cycle at the G0/G1 phase. Clin Exp Pharmacol Physiol 2010;37:605–12.
[36] Morrison RS, Wenzel HJ, Kinoshita Y, Robbins CA, Donehower LA, Schwartzkroin PA. Loss of the p53 tumor suppressor gene protects neurons from kainate-induced cell death. J Neurosci 1996;16:1337–45.
[37] Laptenko O, Prives C. Transcriptional regulation by p53: one protein, many possibilities. Cell Death Differ 2006;13:951–61.
[38] Brooks CL, Gu W. Ubiquitination, phosphorylation and acetylation: the molecular basis for p53 regulation. Curr Opin Cell Biol 2003;15:164–71.
[39] Ashkenazi A, Pai RC, Fong S, Leung S, Lawrence DA, Marsters SA, Blackie C, Chang L, McMurtrey AE, Hebert A, et al. Safety and antitumor activity of recombinant soluble Apo2 ligand. J Clin Invest 1999;104:155–62.
[40] Armeanu S, Lauer UM, Smirnow I, Schenk M, Weiss TS, Gregor M, Bitzer M. Adenoviral gene transfer of tumor necrosis factor-related apoptosis-inducing ligand overcomes an impaired response of hepatoma cells but causes severe apoptosis in primary human hepatocytes. Cancer Res 2003;63:2369–72.
[41] Lemasters JJ, Nieminen AL, Qian T, Trost LC, Elmore SP, Nishimura Y, Crowe RA, Cascio WE, Bradham CA, Brenner DA, et al. The mitochondrial permeability transition in cell death: a common mechanism in necrosis, apoptosis and autophagy. Biochim Biophys Acta 1998;1366(1–2):177–96.
[42] Shang XJ, Yao G, Ge JP, Sun Y, Teng WH, Huang YF. Procyanidin induces apoptosis and necrosis of prostate cancer cell line PC-3 in a mitochondrion-dependent manner. J Androl 2009;30:122–6.
[43] Nam KY, Choi JE, Park JD. Transformation Techniques for the Large Scale Production of Ginsenoside Rg3. Korean J Medicinal Crop Sci 2013;21(5):401–14.